\



Photonic spin Hall effect and terahertz gas sensor via InSb-supported long-range surface plasmon resonance

Jie Cheng(程杰), Gaojun Wang(王高俊), Peng Dong(董鹏), Dapeng Liu(刘大鹏), Fengfeng Chi(迟逢逢), and Shengli Liu(刘胜利)

Citation: Chin. Phys. B, 2022, 31 (**1**): 014205. DOI: 10.1088/1674-1056/ac192a
Journal homepage: http://cpb.iphy.ac.cn; http://iopscience.iop.org/cpb

What follows is a list of articles you may be interested in

Plasmonic sensor with self-reference capability based on functional layer film composed of Au/Si gratings

Jiankai Zhu(朱剑凯), Xiangxian Wang(王向贤), Yunping Qi(祁云平), and Jianli Yu(余建立)
Chin. Phys. B, 2022, 31 (**1**): 014206. DOI: 10.1088/1674-1056/ac1335

Controlled plasmon-enhanced fluorescence by spherical microcavity

Jingyi Zhao(赵静怡), Weidong Zhang(张威东), Te Wen(温特), Lulu Ye(叶璐璐), Hai Lin(林海), Jinglin Tang(唐靖霖), Qihuang Gong(龚旗煌), and Guowei Lyu(吕国伟)
Chin. Phys. B, 2021, 30 (**11**): 114215. DOI: 10.1088/1674-1056/ac0daa

Optical absorption tunability and local electric field distribution of gold-dielectric-silver three-layered cylindrical nanotube

Ye-Wan Ma(马业万), Zhao-Wang Wu(吴兆旺), Yan-Yan Jiang(江燕燕), Juan Li(李娟), Xun-Chang Yin(尹训昌), Li-Hua Zhang(章礼华), and Ming-Fang Yi(易明芳)
Chin. Phys. B, 2021, 30 (**11**): 114207. DOI: 10.1088/1674-1056/ac0785

Solar energy full-spectrum perfect absorption and efficient photo-thermal generation

Zhefu Liao(廖喆夫), Zhengqi Liu(刘正奇), Qizhao Wu(吴起兆), Xiaoshan Liu(刘晓山), Xuefeng Zhan(詹学峰), Gaorong Zeng(曾高荣), and Guiqiang Liu(刘桂强)
Chin. Phys. B, 2021, 30 (**8**): 084206. DOI: 10.1088/1674-1056/ac0696

A novel plasmonic refractive index sensor based on gold/silicon complementary grating structure

Xiangxian Wang(王向贤), Jiankai Zhu(朱剑凯), Yueqi Xu(徐月奇), Yunping Qi(祁云平), Liping Zhang(张丽萍), Hua Yang(杨华), and Zao Yi(易早)
Chin. Phys. B, 2021, 30 (**2**): 024207. DOI: 10.1088/1674-1056/abd690

Photonic spin Hall effect and terahertz gas sensor via InSb-supported long-range surface plasmon resonance

Jie Cheng(程杰)[1,†], Gaojun Wang(王高俊)[1], Peng Dong(董鹏)[2], Dapeng Liu(刘大鹏)[2], Fengfeng Chi(迟逢逢)[1], and Shengli Liu(刘胜利)[1]

[1] *School of Science, New Energy Technology Engineering Laboratory of Jiangsu Province, Nanjing University of Posts and Telecommunications, Nanjing* 210023, *China*
[2] *College of Electronic and Optical Engineering & College of Microelectronics, Nanjing University of Posts and Telecommunications, Nanjing* 210023, *China*

(Received 1 June 2021; revised manuscript received 3 July 2021; accepted manuscript online 30 July 2021)

The photonic spin Hall effect (SHE), featured by a spin-dependent transverse shift of left- and right-handed circularly polarized light, holds great potential for applications in optical sensors, precise metrology and nanophotonic devices. In this paper, we present the significant enhancement of photonic SHE in the terahertz range by considering the InSb-supported long-range surface plasmon resonance (LRSPR) effect. The influences of the InSb/ENZ layer thickness and temperature on the photonic SHE were investigated. With the optimal structural parameters and temperature, the maximal spin shift of the horizontal polarization light can reach up to 2.68 mm. Moreover, the spin shift is very sensitive to the refractive index change of gas, and thus a terahertz gas sensing device with a superior intensity sensitivity of 2.5×10^5 μm/RIU is proposed. These findings provide an effective method to enhance the photonic SHE in the terahertz range and therefore offer the opportunity for developing the terahertz optical sensors based on photonic SHE.

Keywords: surface plasmon resonance, photonic spin Hall effect, InSb, gas sensor

PACS: 42.25.–p, 41.20.Jb, 42.79.–e, 78.20.Ci **DOI:** 10.1088/1674-1056/ac192a

1. Introduction

Photonic spin Hall effect (SHE) is an interesting phenomenon in which the left- and right-circular components shift transversely perpendicular to the refractive index gradient when a light beam propagates through an inhomogeneous medium.[1–3] It is an optical version of SHE in electronic systems, where the roles of the spin photons and refractive index gradient are similar to spin electrons and electric potential, respectively.[1,3] This transverse shift is also called Imbert–Fedorov (IF) shift as it was theoretically predicted by Fedorov and experimentally confirmed by Imbert.[4,5] Generally, the inherent physical mechanism of photonic SHE is believed to be an effective spin–orbit interaction of photons based on the fundamental law of angular momentum conservation.[6,7] Owing to its enormous potential applications in precision metrology and quantum information technology, photonic SHE has attracted increasing attention since its discovery.[8,9] It has also been adopted to identify the layer numbers of graphene,[10] to realize the real-time detection of dynamic chemical reaction,[11] to apply for the optical differential operation and edge detection.[12] Recently, the optical sensor based on the photonic SHE has been proposed.[13–16] However, photonic SHE is a weak effect whose spin-dependent transverse splitting is usually limited to the subwavelength scale. Therefore, it cannot be directly observed with conventional experimental methods, and the successful detection must be incorporated with quantum weak measurements.[17] To facilitate its application, enhancing the photonic SHE has become very significant.

In recent years, several methods and novel materials have been proposed to enhance the photonic SHE, including the Brewster angle,[18] resonant optical tunneling effect,[19] optical pumping,[20] exceptional points in parity–time symmetric systems,[21] two-dimensional atomic crystals[22] and so on. Moreover, surface plasmon resonance (SPR)[23,24] is an effective way to improve the photonic SHE.[15,25–27] For example, Zhou *et al.* presented the enhanced photonic SHE in a simple glass-metal-air structure.[25] Nevertheless, conventional surface plasmon polariton (SPP) is always characterized by the strong absorption loss, inadequate propagation length and shallow penetration depth, which may be detrimental to its further applications. Long-range surface plasmon polariton (LRSPP) is a coupling mode of two SPPs, and it has been demonstrated to have lower loss, narrower angular resonance curves, longer propagation length and greater penetration depth. Based on these advantages, the long-range surface plasmon resonance (LRSPR) has the potential to enhance the photonic SHE. Recently, Tan *et al.* reported that by exciting the LRSPP in a prism-silica-gold-silica structure, the largest spin shift with a 632.8 nm incident Gaussian beam can reach 7.85 μm,[28] which is about 3.5 times larger than the value in conventional SPR configurations.[25] Note that previous reports have focused on the enhancement of photonic SHE in

†Corresponding author. E-mail: chengj@njupt.edu.cn

© 2022 Chinese Physical Society and IOP Publishing Ltd

the visible range based on the excitation of SPP by metals; however, inadequate attentions are paid to the terahertz range. Therefore, investigating the photonic SHE by taking advantage of the LRSPR effect in the terahertz range is highly desirable.

The first and most urgent challenge is to look for suitable materials instead of metals for the excitation and tunneling of terahertz SPPs. Alternative materials can be the semiconductors, whose permittivities in the terahertz region are similar to those of metals in the visible region. Among them, InSb is a semiconductor with a very small energy gap of 0.17 eV and a very large electronic mobility $\sim 7.7\times10^4$ cm$^2\cdot$V$^{-1}\cdot$s^{-1}.[29] In particular, its permittivity can be dynamically tuned by varying the temperature.[30–32] Therefore, InSb is a good candidate to construct the LRSPR configuration in the terahertz region, and the photonic SHE of this InSb-based structure could be flexibly controlled by the temperature.

Epsilon-near-zero (ENZ) metamaterial is a special kind of artificial medium in which the permittivity is close to zero. The enhanced photonic SHE of both transmitted and reflected light can be obtained in a thin ENZ slab.[33,34] In this paper, ENZ material is adopted to be the dielectric layer, and with regard to the requirement of LRSPR effect, InSb material should be surrounded by these two ENZ layers to realize the coupling of two SPPs. We present the significant enhancement of photonic SHE for this InSb-based LRSPR structure in the terahertz region. Under the optimal structural parameters and temperature, the maximum spin shift is found to be 2.68 mm. Finally, the terahertz gas sensor based on the photonic SHE is proposed with a superior intensity sensitivity of 2.5×10^5 μm/RIU. Our research is important for providing an effective way to enhance the photonic SHE in the terahertz region and may offer the opportunity to develop the terahertz sensors based on the photonic SHE.

2. Theory and model

A multilayer symmetric structure composed of air, InSb and ENZ slab is proposed in Fig. 1. The incident light is a Gaussian beam whose frequency is 1 THz with the beam waist of 30λ. For simplicity, the thickness of the ENZ layer and InSb are defined as d_2 and d_3, respectively. The relative dielectric constant of the ENZ slab is set to be 0.01.[33,34] The permittivity of the InSb semiconductor can be described well by the following Drude model:[35]

$$\varepsilon(\omega,T)=\varepsilon_\infty-\frac{\omega_{\rm p}^2(T)}{\omega[\omega+{\rm i}\Gamma(T)]}, \tag{1}$$

where $\varepsilon_\infty=15.75$ is the high-frequency permittivity, $\omega_{\rm p}=\sqrt{Ne^2/(\varepsilon_0 m^*)}$ is the plasma frequency and the scattering rate Γ is related to the carrier mobility μ by $\Gamma(T)=1/(m^*\mu(T)/e)$. The carrier effective mass m^* in InSb is $0.015m_0$, where $m_0=9.1\times10^{-31}$ kg is the electron mass. The carrier mobility μ can be obtained by the empirical formula $\mu=77000(T/300)^{-1.66}$ cm$^2\cdot$V$^{-1}\cdot$s^{-1}.[29] The relationship between the charge carrier concentration N and temperature T can be expressed as[36]

$$N=2.9\times10^{11}(2400-T)^{0.75}\left(1+2.7\times10^{-4}T\right)T^{1.5}\times\exp\left(-\frac{0.129-1.5\times10^{-4}T}{k_{\rm B}T}\right). \tag{2}$$

Therefore the permittivity of InSb can be effectively tuned by temperature, and firstly the temperature is taken to be 300 K in the following discussion.

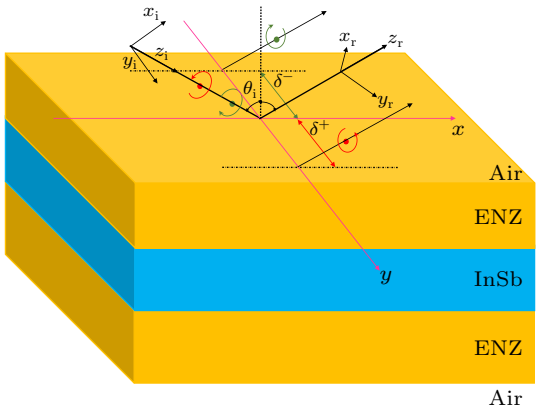


Fig. 1. Schematic of the photonic SHE in the multilayer LRSPR structure of air–ENZ–InSb–ENZ–air. δ^+ and δ^- denote the transverse shifts of left- and right-circularly polarized light beam centroid, respectively.

A monochromatic Gaussian beam is incident from the air to the surface of the multilayer structure with an incident angle $\theta_{\rm i}$, and the photonic SHE of reflected light occurs due to the excitation of LRSPR, manifesting itself as the opposite shifts of the left- and right-circularly polarized light. In our configuration of Fig. 1, the incident plane is x–z and the spin shift is along the y-axis. We consider an incident Gaussian beam with angular spectrum of

$$\tilde{\boldsymbol{E}}_{\rm i}=\frac{w_0}{\sqrt{2\pi}}\exp\left[-\frac{(k_x^2+k_y^2)w_0^2}{4}\right], \tag{3}$$

in which w_0 is the beam waist, and k_x and k_y are the wave vector components along the x and y directions, respectively. By matching the boundary condition, the angular spectrum of the reflected beam can be expressed as[37]

$$\begin{bmatrix}\tilde{\boldsymbol{E}}_{\rm r}^{\rm H}\\ \tilde{\boldsymbol{E}}_{\rm r}^{\rm V}\end{bmatrix}=\begin{bmatrix}r_{\rm p} & \dfrac{k_{\rm ry}\cot\theta_{\rm i}(r_{\rm p}+r_{\rm s})}{k_0}\\ -\dfrac{k_{\rm ry}\cot\theta_{\rm i}(r_{\rm p}+r_{\rm s})}{k_0} & r_{\rm s}\end{bmatrix}\begin{bmatrix}\tilde{\boldsymbol{E}}_{\rm i}^{\rm H}\\ \tilde{\boldsymbol{E}}_{\rm i}^{\rm V}\end{bmatrix}, \tag{4}$$

in which $\tilde{\boldsymbol{E}}_{\rm r}^{\rm H,V}$ and $\tilde{\boldsymbol{E}}_{\rm i}^{\rm H,V}$ are the H and V components of the angular spectrum with the reflected and incident beams, respectively. k_0 is the wave number in free space and $k_{\rm ry}$ is the y component of the reflected wave vector. $r_{\rm p}$ and $r_{\rm s}$ are Fresnel

reflection coefficients for p and s waves, which can be determined by a 2×2 transfer matrix[37]

$$M = T_{1\to2}P_2T_{2\to3}P_3\cdots P_mT_{m\to m+1}, \tag{5}$$

where

$$T_{m\to m+1} = \frac{1}{t_{m\to m+1}}\begin{bmatrix} 1 & r_{m\to m+1} \\ r_{m\to m+1} & 1 \end{bmatrix}$$

is the transmission matrix from m layer to $(m+1)$ layer, and

$$P_m = \begin{bmatrix} \exp(\mathrm{i}k_{mz}d_m) & 0 \\ 0 & \exp(-\mathrm{i}k_{mz}d_m) \end{bmatrix}$$

is the propagation matrix for the m layer with the thickness of d_m. The Fresnel reflection coefficients (r_p and r_s) are given by the elements of the transfer matrix: $r_{\mathrm{p,s}} = M_{21}/M_{11}$. Then the Fresnel reflectance can be calculated for p and s polarizations as $R_{\mathrm{s,p}} = |r_{\mathrm{s,p}}|^2$.

For a Gaussian incident light, the two circular components of the reflected field can be given as[28]

$$E^{\pm}_{\mathrm{H,V}} \propto \frac{w_0}{w}\exp\left[-\frac{x_\mathrm{r}^2+y_\mathrm{r}^2}{w}\right] \times\left[r_\mathrm{p} - \frac{2\mathrm{i}x_\mathrm{r}}{k_0w}\frac{\partial r_\mathrm{p}}{\partial\theta} \mp \frac{2y_\mathrm{r}\cot\theta_\mathrm{i}}{k_0w}(r_\mathrm{p}+r_\mathrm{s})\right], \tag{6}$$

in which $w = w_0\left[1+\left(2z_\mathrm{r}/k_0w_0^2\right)^2\right]^{1/2}$, and $\pm$ denotes the left- and right-circularly polarized components. Then the spin shift of the reflected light can be defined as

$$\delta^{\pm}_{\mathrm{H,V}} = \frac{\iint y\left|\boldsymbol{E}^{\pm}_{\mathrm{H,V}}\right|^2\mathrm{d}x\mathrm{d}y}{\iint\left|\boldsymbol{E}^{\pm}_{\mathrm{H,V}}\right|^2\mathrm{d}x\mathrm{d}y}. \tag{7}$$

If we consider the first-order Taylor series and neglect the high-order infinitesimal of the Fresnel coefficients, the spin-dependent transverse shifts can be derived as[28]

$$\delta^{\pm}_{\mathrm{H}} = \mp\frac{k_0w_0^2\mathrm{Re}(1+r_\mathrm{s}/r_\mathrm{p})\cot\theta_\mathrm{i}}{k_0^2w_0^2+\left|\dfrac{\partial\ln r_\mathrm{p}}{\partial\theta_\mathrm{i}}\right|^2+\left|(1+r_\mathrm{s}/r_\mathrm{p})\cot\theta_\mathrm{i}\right|^2}, \tag{8}$$

$$\delta^{\pm}_{\mathrm{V}} = \mp\frac{k_0w_0^2\mathrm{Re}(1+r_\mathrm{p}/r_\mathrm{s})\cot\theta_\mathrm{i}}{k_0^2w_0^2+\left|\dfrac{\partial\ln r_\mathrm{s}}{\partial\theta_\mathrm{i}}\right|^2+\left|(1+r_\mathrm{p}/r_\mathrm{s})\cot\theta_\mathrm{i}\right|^2}. \tag{9}$$

Note that the spin shifts for left- and right-circularly polarized light are the same in magnitude but opposite in sign, and the value is determined by the ratio between r_p and r_s. When the LRSPR is excited by H polarization light, r_p has a minimum value around the resonant angle, while r_s changes slightly, which will lead to a large ratio of $|r_\mathrm{s}|/|r_\mathrm{p}|$ and then a giant spin shift $\delta^{\pm}_{\mathrm{H}}$.[25] On the contrary, there is no plasmon field for the V polarized incident beam, so that the corresponding spin shift is relatively small.[25] Therefore in the next section we will explore the behavior of photonic SHE for H polarized light due to the LRSPR effect.

3. Results and discussion

The LRSPP is the symmetric mode of surface electromagnetic wave which generally exists and propagates along the interface of metal (semiconductor) and dielectric medium. In addition, the strength of LRSPP is extremely sensitive to the thickness of metal (semiconductor) and dielectric layers.[28] Figure 2 displays the corresponding reflection spectra with the incident angles under different thicknesses of ENZ slab (d_2) and InSb (d_3) layer. It can be clearly seen from Fig. 2(a) that there are two resonant peaks in the R_p reflection curve; the left one with narrower resonance dip and longer penetration depth stands for LRSPP, while the right one is caused by short-range SPP. We find that an increased thickness of the ENZ slab has little effect on the penetration depth of LRSPR, but the resonance angle decreases slightly. When the thickness of the InSb layer decreases from 50 nm to 30 nm, the resonance position of LRSPR moves towards a smaller angle, accompanied by the increased penetration depth. Unlike R_p, R_s changes monotonically with increasing the incident angle and it even keeps almost stable under a large incident angle. According to Eq. (8), the transverse spin shift of reflected light for the H polarization beam is determined by the value of $|r_\mathrm{s}|/|r_\mathrm{p}|$ ratio, and a large ratio around the resonant dip of LRSPR would result in the giant spin shift $\delta^{\pm}_{\mathrm{H}}$. Here we present the ratio of $|r_\mathrm{s}|/|r_\mathrm{p}|$ under different thicknesses of the ENZ slab and InSb layers in Fig. 2(c). It is found that the $|r_\mathrm{s}|/|r_\mathrm{p}|$ ratio is affected by the thicknesses of both the ENZ and InSb layers, and then the photonic SHE would be accordingly tuned. In our InSb-based LRSPR structure, the InSb layer is responsible for exciting the terahertz SPPs. Hence, we will firstly fix the thickness of ENZ slab to 50 μm and analyze the role of InSb thickness on the spin shift $\delta^{\pm}_{\mathrm{H}}$.

Figure 3(a) describes the impacts of InSb thickness and incident angle on the photonic SHE. For the sake of convenience, we only present the spin shift of the left-circularly polarized component δ^{+}_{H}. It can be found that the spin shift undergoes huge changes near the resonance angle, and the optimal incident angle which corresponds to the maximal value of δ^{+}_{H} varies with the thickness of the InSb layer. As shown in Fig. 3(b), the optimal incident angle increases linearly from 6.2° to 7.5° with increasing the thickness of InSb to 600 nm. However, the spin shift firstly increases to a maximum value and then decreases sharply with the increment of InSb thickness, which may be due to the weak coupling and even the decoupling of two SPPs. This phenomenon is consistent with the variation of photonic SHE versus the thickness of the gold layer in the LRSPR structure of prism-silica-gold-silica.[28] Consequently, there should be an optimal parameter of InSb

thickness where the giant spin shift can be achieved due to the excitation of strong LRSPR. Obviously, the optimal thickness of InSb is about 450 nm, and the corresponding spin shift can reach the largest value of 1.83 mm under the optimal incident angle of 7.1° (in Fig. 3(c)). It can be clearly seen from Fig. 3(d) that the R_p curve exhibits an obvious dip and the strong LRSPR effect is indeed excited with the InSb thickness of 450 nm. Based on the above discussion, one can draw a conclusion that such a giant spin shift in the terahertz region is attributed to the InSb-supported LRSPR effect.

Table 1. The maximum values of spin shifts, as well as the optimal incident angle and the thickness of ENZ and InSb layers.

Fixed thickness of ENZ slab (μm)	Maximal spin shift (mm)	Optimal thickness of InSb layer (nm)	Optimal incident angle (°)
30	1.83	260	7.1
40	1.83	375	7.2
50	1.83	450	7.1
60	1.79	490	7.0
70	1.73	525	6.9

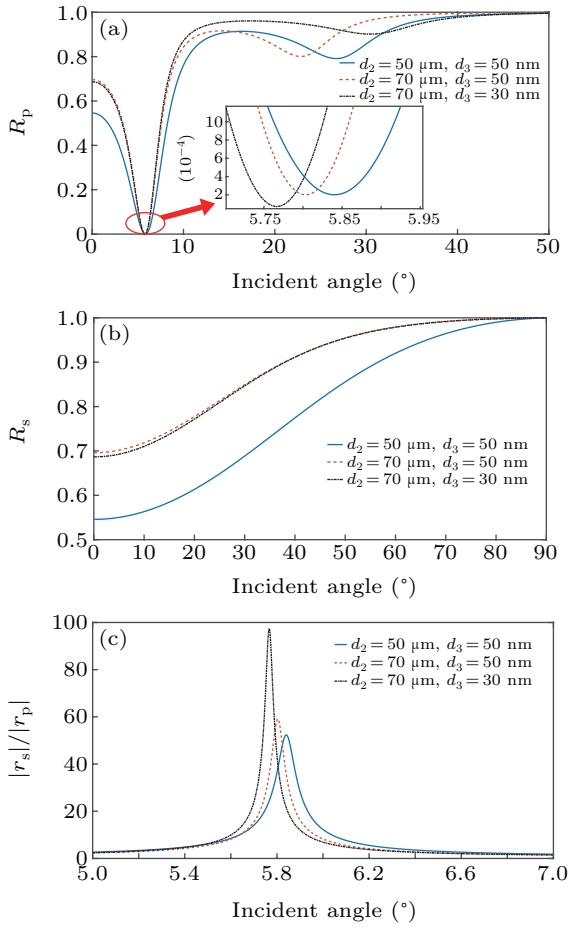


Fig. 2. Impact of the thickness of the ENZ slab and InSb layer on the reflectance (a) $R_p = |r_p|^2$, (b) $R_s = |r_s|^2$ and (c) the ratio $|r_s|/|r_p|$ under the condition of LRSPR.

Note that the above discussions are based on the ENZ slab thickness of 50 μm. To study the influence of the thickness of the ENZ layer on the photonic SHE, we choose other values of ENZ layer thickness (i.e., 30 μm, 40 μm, 60 μm, and 70 μm). The maximal spin shifts, as well as the corresponding incident angle and the optimal thickness of the InSb layer, are given in Table 1. For different ENZ layer thicknesses, the optimal incident and optimal InSb thickness vary, and consequently different enhancements of photonic SHE are achieved. It is clearly seen that, as the thickness of ENZ slab varies from 30 μm to 50 μm, the maximum value of spin shift is almost stable (∼ 1.83 mm). As the ENZ layer thickness keeps increasing (60 μm and 70 μm), the maximal spin shift decreases sharply. Therefore, the photonic SHE is affected by the thicknesses of both the ENZ layer and InSb layer, and the optimal parameter setup is found to generate the largest spin shift.

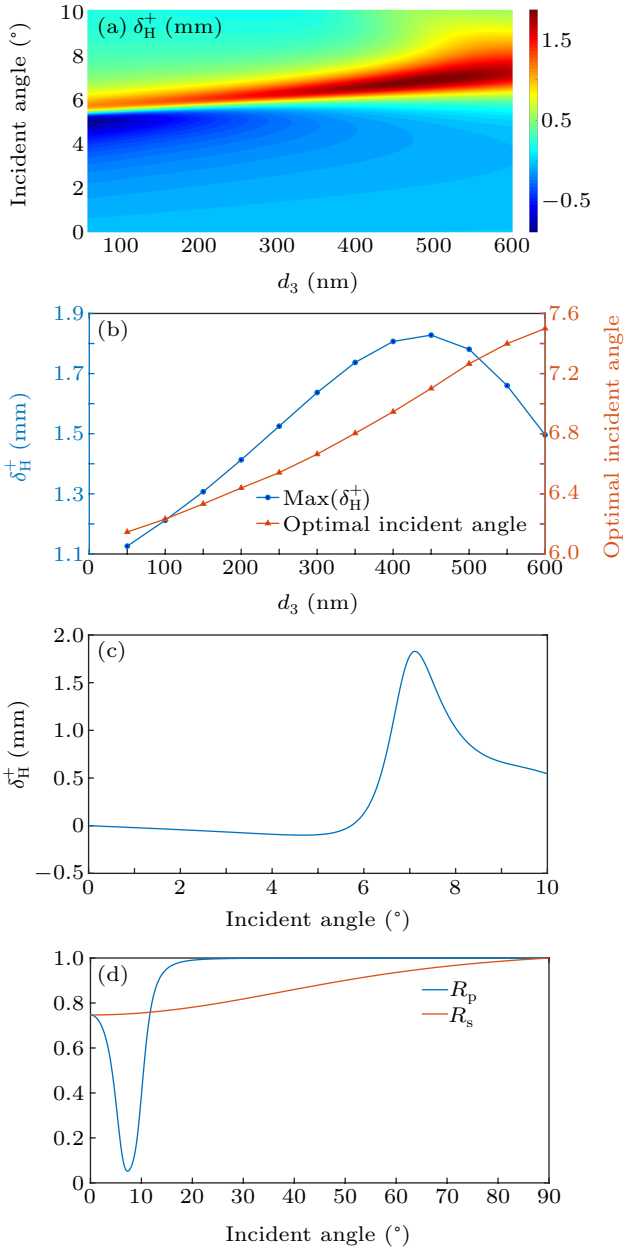


Fig. 3. (a) Spin shifts as functions of the InSb thickness and incident angle. (b) The maximal spin shift δ_H^+ and optimal incident angle varying with the thickness of InSb layer. (c) Largest spin shift δ_H^+. (d) The corresponding reflection spectra under optimal conditions.

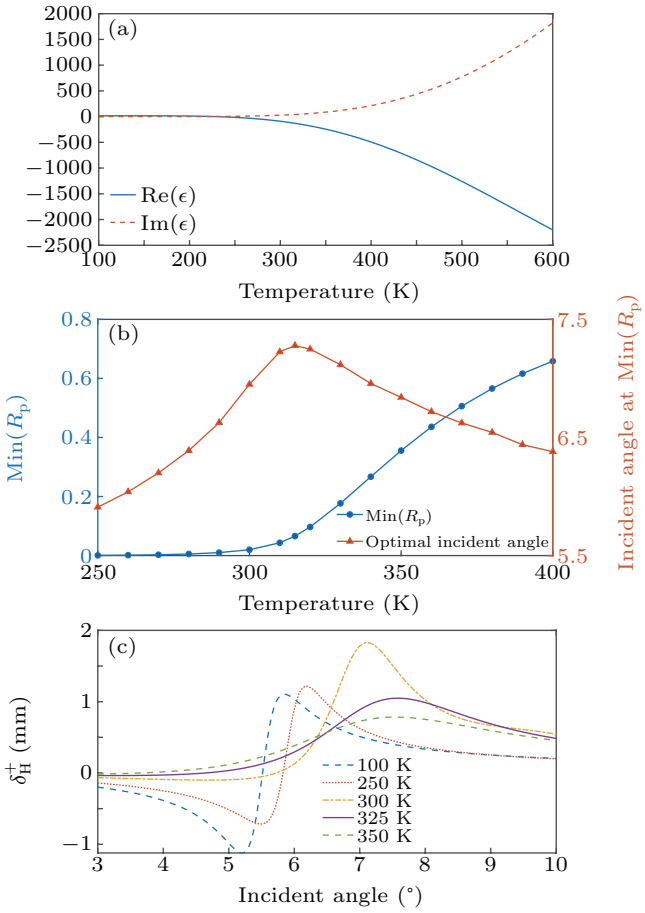


Fig. 4. (a) The permittivity of InSb for different temperatures at 1 THz. (b) Variations of the minimum value of R_p and corresponding incident angle with the temperature. (c) The spin shift δ_H^+ versus the incident angle with different temperatures. Here $d_2 = 50$ μm and $d_3 = 450$ nm.

Considering Eq. (1), temperature is a tunable parameter to control the permittivity of InSb, and therefore the behavior of photonic SHE would be accordingly modulated by temperature. The dependence of InSb permittivity on the temperature at 1 THz is shown in Fig. 4(a). It can be seen that both the real and imaginary parts of InSb permittivity stabilize to be a tiny value when the temperature is smaller than 260 K. As the temperature continues to increase, the real term becomes negative and the imaginary one increases to be a large positive value. In order to explore the influence of temperature on LRSPP, we provide the relationship between the minimum value of R_p and the corresponding resonant angle with different temperatures in Fig. 4(b). It is demonstrated that the minimum value of R_p changes slightly at low temperature, owing to the stable behavior of InSb permittivity. Then it undergoes the rapid increase with increasing the temperature. For example, the minimum value of R_p increases to 0.66 at 400 K, which may indicate the decoupling of two SPPs at high temperature. However, the corresponding resonant angle (i.e., incident angle at Min(R_p)) increases to a maximum value of 7.3° at about 315 K and then decreases with the high temperature. Figure 4(c) displays the effect of temperature on the spin shift. It is pointed out that the maximum value of spin shift can be flexibly controlled by the temperature, accompanied by the variation of the optimal incident angle. There is an optimal temperature to obtain the giant spin shift around the resonance angle of LRSPR. The optimal temperature is about 300 K under the incident angle of 6.9° when the thickness of ENZ slab and InSb layer are 50 μm and 450 nm, respectively. Consequently, temperature can be used as a tuning factor for photonic SHE, and to achieve the giant spin shift, the incident angle should be accordingly changed with temperature in the practical application of photonic devices.

According to the Eq. (8), the beam waist would affect the value of spin shifts. Hence the influence of beam waist on the tunability of spin shifts has also been investigated, as illustrated in Fig. 5. It is clearly seen that the spin shift increases with the increase of beam waist. For example, if we fix the beam waist of 30λ, the maximum spin shift is about 1.83 mm. When the beam waist equals 90λ, the maximum value of 2.50 mm can be obtained. However, when we continue to increase the beam waist, which is much larger than the incident wavelength, the effect of the beam waist on the photonic SHE becomes relatively weak. Under the optimal parameter setup, the maximum spin shift with a 1 THz incident beam reaches 2.68 mm, which is about 340 times larger than the spin shift induced by LRSPR for the incident wavelength of 632.8 nm.[28]

As a unique physical mechanism, the SPR effect has taken a renowned position in the field of sensing technology. In recent years, SPR sensing methodology has supported a wide range of applications in the fields of food safety, drug testing, medical analysis, environmental monitoring and so on.[38–40] Until now, most SPR-based sensors have been focused in the visible and infrared ranges by using the conventional noble metals like gold and silver. The research into terahertz sensors remains at the initial stage, although the combination of terahertz plasmonics and the high sensitivity of SPR holds great promise in terahertz sensing. Recently, Purkayastha *et al.* proposed a SPR-based sensor in terahertz frequency using a free-standing doped graphene monolayer, and this sensor shows ultrahigh sensitivity of 34.11 °/RIU along with an ultrahigh figure of merit.[41] A terahertz sensor based on a graphene-Bragg reflector composite structure is designed, and the maximal sensitivity of 407.36 °/RIU is obtained.[42] In fact, the terahertz gas sensor still has great potential because the vibrational and rotational energy of most gas molecules lie in the terahertz range. Here, we propose a terahertz gas sensor based on photonic SHE induced by the excitation of InSb-supported LRSPP. Therein, the lowest air layer in Fig. 1 can be replaced to fill the sensing gas molecules.

According to the intensity-based shift sensing scheme, the gas sensor is conducted by setting a fixed working angle as shown in Fig. 6. The intensity sensitivity can be defined as $S_{\delta_H^+} = \Delta\delta_H^+/\Delta n_g$, where $\Delta\delta_H^+$ is the difference of spin shift caused by a refractive index change of gas Δn_g. We find that the spin shift of photonic SHE is very sensitive to the refractive index variation of gas, and a high intensity sensitivity of 2.5×10^5 μm/RIU can be obtained, which is about 38 times higher than that of the metal SPR structure.[15] It should be noted that in our work the initial spin shift is applied to calculate the sensing sensitivity without any amplification technique. Nevertheless, its sensitivity is 2.5 times larger than that of a photonic SHE-based sensor using a signal enhancement method of weak measurement.[16] Therefore the proposed structure shows a superior sensing performance, and the gas sensor has potential applications in toxic monitoring, explosive detection and pollution control.

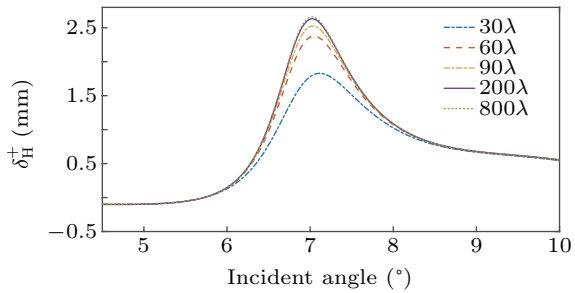


Fig. 5. The spin shift versus the incident angle with different beam waists. Here $d_2 = 50$ μm and $d_3 = 450$ nm.

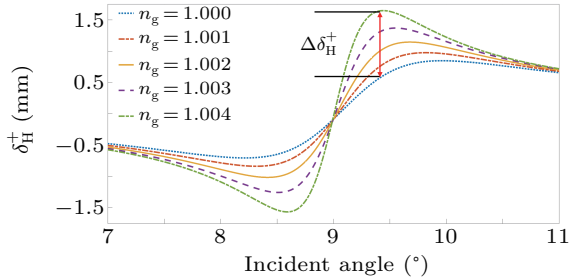


Fig. 6. The intensity sensitivity for the gas sensor of InSb-based LRSPR structure.

4. Conclusion

In summary, we have reported the enhanced photonic SHE in the terahertz range while the InSb-supported LRSPR is excited. The thickness of the InSb layer has a major impact on the value of spin shift. In view of the intimate relationship between optical properties of InSb and temperature, the spin shift can be dynamically tuned by temperature. Under the condition of optimal parameters, the giant spin shift of 2.68 mm is generated. Finally, the spin shift is quite sensitive to the refractive index changes of measured gases. Therefore, the proposed LRSPR structure can be applied to the design of the terahertz gas sensor, and the intensity sensitivity is about 2.5×10^5 μm/RIU, demonstrating a superior sensing performance. Our research provides a significant design guide for developing terahertz nanophotonic devices based on the LR-SPR effect.

Acknowledgments

Project supported by the National Natural Science Foundation of China (NSFC) (Grant No. 12175107), Open Project of National Laboratory of Solid State Microstructures of Nanjing University (Grant No. M32022), and the Natural Science Foundation of Nanjing University of Posts and Telecommunications (Grant No. NY220030).

References

[1] Onada M, Murakami S and Nagaosa N 2004 *Phys. Rev. Lett.* **93** 083901
[2] Sinova J, Culcer D, Niu Q, Sinitsyn N A, Jungwirth T and Macdonald A H 2004 *Phys. Rev. Lett.* **92** 126603
[3] Bliokh K Y, Rodríguez-Fortuño F J, Nori F and Zayats A V 2015 *Nat. Photon.* **9** 796
[4] Fedorov F I 2013 *J. Opt.* **15** 014002
[5] Imbert C 1972 *Phys. Rev. D* **5** 787
[6] Bliokh K Y, Rodríguez-Fortuño F J, Nori F and Zayats A V 2015 *Nat. Photon.* **9** 796
[7] Cardano F and Marrucci L 2015 *Nat. Photon.* **9** 776
[8] Chi C, Jiang Q, Liu Z X, Zheng L H, Jiang M L. Zhang H, Lin F, Shen B and Fang Z Y 2021 *Sci. Adv.* **7** eabf8011
[9] Ling X H, Zhou X X, Huang K and Liu Y H 2017 *Rep. Prog. Phys.* **80** 066401
[10] Zhou X X, Ling X H, Luo H L and Wen S C 2012 *Appl. Phys. Lett.* **101** 251602
[11] Wang R S, Zhou J X, Zeng K M, Chen S Z, Ling X H, Shu W X, Luo H L and Wen S C 2020 *APL Photon.* **5** 016105
[12] He S S, Zhou J X, Chen S Z, Shu W X, Luo H L and Wen S C 2020 *Opt. Lett.* **45** 877
[13] Li N X, Tang T T, Li J, Luo L, Li C Y, Shen J and Yao J Q 2019 *J. Magn. Magn. Mater.* **484** 445
[14] Jiang X, Tang J, Li Z F, Liao Y L, Jiang L Y, Dai X Y and Xiang Y J 2019 *J. Phys. D: Appl. Phys.* **52** 045401
[15] Jiang X, Wang Q K, Guo J, Chen S Q, Dai X Y and Xiang Y J 2018 *Plasmonics* **13** 1467
[16] Zhou X X, Sheng L J and Ling X H 2018 *Sci. Rep.* **8** 1221
[17] Hosten O and Kwiat P 2008 *Science* **319** 787
[18] Luo H L, Zhou X X, Shu W X, Wen S C and Fan D Y 2011 *Phys. Rev. A* **84** 043806
[19] Jiang X, Wang Q K, Guo J, Zhang J, Chen S Q, Dai X Y and Xiang Y J 2018 *J. Phys. D: Appl. Phys.* **51** 145104
[20] Dong P, Cheng J, Da H X and Yan X H 2020 *New J. Phys.* **22** 113007
[21] Zhou X X, Lin X, Xiao Z C, Low T, Al'u A, Zhang B L and Sun H D 2019 *Phys. Rev. B* **100** 115429
[22] Dong P, Wang G J and Cheng J 2021 *Chin. Phys. B* **30** 034202
[23] Li Z W, Li Y, Han T Y, Wang X L, Yu Y, Tay B, Liu Z and Fang Z Y 2017 *ACS Nano* **11** 1165
[24] Zheng L H, Liu Z X, Liu D L, Wang X G, Li Y, Jiang M L, Lin F, Zhang H, Shen B, Zhu X, Gong Y J and Fang Z Y 2021 *Nat. Commun.* **12** 291
[25] Zhou X X and Ling X H 2016 *IEEE Photon. J.* **8** 4801108
[26] Xiang Y J, Jiang X, You Q, Guo J and Dai X Y 2017 *Photonics Res.* **5** 467
[27] Wang Q K, Jiang X, Wang X, Dai X Y and Xiang Y J 2017 *IEEE Photon. J.* **9** 6102610
[28] Tan X J and Zhu X S 2016 *Opt. Lett.* **41** 2478
[29] Madelung O 1964 *Physics of III-V Compounds* (New York)
[30] Tang Q Y, Wang Q, Zhang D W, Wang Z F and Huang Y S 2014 *Superlattice. Microst.* **75** 955
[31] Rivas J G, Janke C, Bolivar P H and Kurz H 2005 *Opt. Express* **13** 847
[32] Wang P X, Wan B F, Peng H M, Hai Y M, Zhang F and Zhang D 2021 *Opt. Quant. Electron* **53** 113

[33] Zhu W G and She W L 2015 *Opt. Lett.* **40** 2961
[34] Luo L and Tang T T 2017 *Superlattice. Microst.* **109** 259
[35] Sánchez-Gil J A and Rivas J G 2006 *Phys. Rev. B* **73** 205410
[36] Oszwaldowski M and Zimpe M 1988 *Phys. Chem. Solids* **49** 1179
[37] Luo H L, Ling X H, Zhou X X, Shu W X, Wen S C and Fan D Y 2011 *Phys. Rev. A* **84** 033801
[38] Piliarik M, Parova L and Homola J 2009 *Biosens. Bioelectron.* **24** 1399
[39] Yoo H, Shin J, Sim J, Cho H and Hong S 2020 *Biosens. Bioelectron.* **168** 112561
[40] Conteduca D, Dell'Olio F, Innone F, Ciminelli C and Armenise M N 2016 *Opt. Laser Technol.* **77** 151
[41] Purkayastha A, Srivastava T and Jha R 2016 *Sensor Actuat. B-Chem.* **227** 291
[42] Tang J, Ye Y Y, Xu J, Zheng Z W, Jin X L, Jiang L Y, Jiang J and Xiang Y J 2020 *Nanomaterials* **10** 500